ELSEVIER

Catalysis Today 57 (2000) 313–322

CATALYSIS TODAY

www.elsevier.com/locate/cattod

Characterization of cobalt-impregnated VPO catalysts

L.M. Cornaglia *, C.R. Carrara, J.O. Petunchi[1], E.A. Lombardo

Instituto de Investigaciones en Catálisis y Petroquímica, INCAPE (FIQ, UNL-CONICET), Santiago del Estero 2829, 3000 Santa Fe, Argentina

Abstract

Cobalt-impregnated VPO catalysts containing 1–6% of the metal by weight were prepared. The catalytic tests showed that cobalt impregnation significantly increased the overall activity while slightly decreasing the maleic anhydride selectivity. To investigate the origin of the cobalt effect, the solids were characterized using XRD, Raman spectroscopy, FT-IR, TPR and XPS. No structural effects were detected through XRD. TPR showed that the non-equilibrated catalysts contain cobalt oxides which react with the VPO solids to yield a hard to reduce system. Non-equilibrated umpromoted and promoted (low cobalt loadings) catalysts contain small proportions of V(V) phases. After several 100 h on stream, the only phase detected in all cases was V(IV) vanadyl pyrophosphate. The surface oxidation state of vanadium was V(IV). The maleic anhydride yield correlates with the increased exposure of cobalt on the catalysts surface.

Keywords: *n*-Butane oxidation; Maleic anhydride; VPO; Promoters; Cobalt

1. Introduction

Short-chain alkanes with low market value entice research to develop creative ways to transform them into highly priced chemicals. One possible route is selective oxidation. Unfortunately though, there are few selective catalysts for the oxidation of alkanes. A few examples cited in the literature include the dehydrogenation of alkanes over V–Mg oxides [1], the oxidation of propane to acrolein over Bi–Ag–V–Mg oxides [2], and the only successful industrial process, the oxidation of *n*-butane to maleic anhydride using vanadium–phosphorus oxides (VPO) [3].

The origin of this unique ability of the VPO system to produce this 14-electron oxidation has been a matter of intense research for the last 20 years [3–14]. It is generally agreed upon that the best catalyst precursor is $VOHPO_4{\cdot}0.5H_2O$ which is converted to $(VO)_2P_2O_7$ during activation. In-situ studies using techniques such as NMR, Raman spectroscopy and XRD, have evidenced the presence of V(V)-containing phases in laboratory catalysts. Among them, several $VOPO_4$ phases have been claimed as necessary for the catalytic act [6,7,15]. However, these phases have never been detected in the so-called equilibrated catalysts that have been on stream for over several 100 h [9,16,17]. Maybe, as suggested by several authors, the V(IV)/V(V) couple is formed on the $(VO)_2P_2O_7$ surface of the highly crystalline equilibrated catalysts [10,16,17].

All the industrial catalysts contain promoters of different kinds. Cations such as Ce, Cd, Ni, Zn, Bi, Cu, Li, V, Zr, Mg, Ti, La, Mo, Nb, B, Fe and Cr have

* Corresponding author. Tel.: +54-42-4536861; fax: +54-42-4536861.
E-mail address: nfisico@fiqus.unl.edu.ar (L.M. Cornaglia).

[1] Our recognition and gratitude to Prof. Juan Petunchi for his lifelong lasting contribution to catalysis.

0920-5861/00/$ – see front matter
PII: S0920-5861(99)00342-9

been mainly reported in patents [14], although a few articles have been published in the open literature.

Hutchings [14] points out that the major feature of the most widely reported promotional effects is of a structural nature. He also adds that the promoters play two different structural roles: (i) they allow the formation of the required VPO compounds while impairing the appearance of "deleterious phases", and (ii) they participate in solid solutions which regulate the catalytic properties of the VPO formulations.

Bej and Rao [18] studied the simultaneous addition of Mo and Ce and reported good yields under severe operating conditions. Zazhigalov et al. [19] and Haber et al. [20] studied alkaline and alkaline earth additives. Their goal was to achieve a fine control of the acid–base properties of the surface. Their catalysts, however, did not show a significant improvement in performance. Cheng [21] modified the P/V ratio and added both In and TEOS (tetraethylorthosilicate) to the VPO formulations. He concluded that the promoters drastically decrease both the thickness of platelets in the layered morphology, and their crystallite sizes. Sananes et al. [22] noticed that the addition of either Zn, Zr or Ti increased the molar yield to maleic anhydride in non-equilibrated catalysts.

Chromium-doped catalysts have been studied by Harrouch Batis et al. [23]. They found a strong surface enrichment of chromium in Cr-doped aqueous catalysts which was deleterious for the production of maleic anhydride. The same metal was added to the VPO system by McCormick et al. [24]. They found that the promoter atoms affect the layer linkages in the vanadyl pyrophosphate.

Hutchings and Higgins [25] used a simple kinetic analysis to gauge the effect of a dozen elements upon the catalytic performance. Their main conclusion was that only Mo and Co showed a promotional effect, increasing the product yield per unit surface area. The authors proposed that those cations have an electronic effect that induces the fast desorption of maleic anhydride limiting its overoxidation. Hutchings et al. [26] found that the addition of Co modifies both the bulk and the surface V(V)/V(IV) ratios. These ratios in turn affect the formation of maleic anhydride.

In this work we have studied the role of cobalt-impregnated on the VPO precursors. The evolution of the added Co during phase transformation and throughout equilibration was monitored using several spectroscopic techniques, together with temperature-programmed reduction and plug-flow reaction measurements of catalytic performance.

2. Experimental

2.1. Precursor synthesis

Five grams of V_2O_5 were reduced with 30 ml of isobutanol and 20 ml of benzyl alcohol under reflux for 3 h. Orthophosphoric acid (100%) was then added to obtain the desired P/V ratio in the solid and the solution refluxed for 2 h. The suspension obtained was filtered and the solid dried at 390 K in air for 24 h.

The cobalt (as cobalt acetate) was impregnated on the precursor, VPCo*x*I (where *x* represents wt.% of Co and I stands for impregnated). The impregnation solutions contained the required amount of cobalt acetate in 30 ml of isobutanol. After impregnation, the solvent was evaporated at 310 K, and the wet solid dried at 390 K in air. The final Co content of all of the preparations was determined by atomic absorption.

2.2. Catalyst activation

The catalysts were activated in two steps:

1. A fixed-bed reactor containing 1.0 g of precursor with particle size in the 170–250 μm range (Tyler 60–80 mesh) was heated up to 603 K while flowing a mixture of 0.75% *n*-butane in air with a gas hourly space velocity (GHSV) of 900 h^{-1}. The temperature was kept constant at 603 K for 3 h. Those catalysts which only underwent this treatment are here called non-equilibrated catalysts.
2. The *n*-butane concentration was increased to 1.5% while still maintaining the GHSV at 900 h^{-1}. The temperature was raised until either 80% conversion or the maximum allowable temperature of 703 K was reached. Then, the GHSV was raised to 2500 $h^{-1}$and the temperature was slowly increased with the limitation that conversion never exceeded 80%. The catalytic data reported here were measured over solids that did not show any change in activity and selectivity *after* at least 500 h on stream (equilibrated catalysts). At this point when the reaction temperature was randomly

varied up and down, reproducible values of activities and selectivities were obtained.

2.3. Catalyst characterization

X-ray diffraction. The measurements were made with a Shimadzu XD-D1-ray diffractometer, using Nickel-filtered Cu Kα radiation with a scanning rate of $1^\circ\,min^{-1}$.

Laser Raman spectroscopy (LRS). The Raman spectra were recorded with a Jasco Laser Raman spectrometer model TRS-600-SZ-P, equipped with a CCD (charge coupled device) with the detector cooled to about 153 K using liquid N_2. The excitation source was the 514.5 nm line of a Spectra 9000 Photometrics Ar ion laser. The laser power was set at 30 mW. All the spectra were recorded with the samples under ambient conditions. The powdered solid was pressed into a thin wafer about 1 mm thick.

Infrared spectroscopy. The IR spectra were obtained at room temperature using a Shimadzu FT-IR-8101M spectrometer. The precursor samples were prepared using Fluorolube as the support placed between two KBr windows. The activated samples were prepared in the form of pressed wafers (ca. 2 wt.% sample in KBr).

Temperature-programmed reduction (TPR). The TPR experiments were performed in an Ohkura TP-20022S instrument equipped with a thermal conductivity detector (TCD). Hundred milligrams of samples were used and the reducing gas was a 5% H_2–Ar stream, with a heating rate of $10\,K\,min^{-1}$ up to 1023 K.

X-ray photoelectron spectroscopy. The XPS measurements were carried out using an ESCA750 Shimadzu electron spectrometer. Non-monochromatic Mg Kα X-ray radiation was used. The anode was operated at 8 kV and 30 mA and the pressure in the analysis chamber was about 2×10^{-6} Pa. The data were collected using an ESCAPAC 760 computer interfaced to the spectrometer and analyzed with the Googly software developed at the University of Pittsburgh. The surface atomic ratio were calculated using the areas under the Co $2p_{1/2}$, V $2p_{3/2}$, O 1s and P 2p peaks, the Scofield photoionization cross-sections, the mean free paths of the electrons and the instrumental function which was given by the ESCA manufacturer.

The binding energies (BE) were referred to the C 1s signal (284.6 eV). Curve fitting was performed using a Levenberg-Marquardt NLLSCF routine. The background contribution was considered assuming an integral type background which was included in the basic shape of each peak. Account has been taken in the presence of $K_{\alpha3}$ and $K_{\alpha4}$ spectral lines of the large O 1s signal. These satellite peaks are 8.4 and 10.2 eV down-shifted from the O 1s main peak and overlap the V $2p_{1/2}$ signal. Since the resolution of the V $2p_{1/2}$ is poorer than that of the V $2p_{3/2}$ level, we preferably used the latter BEs and widths for comparison with literature data. The V 2p doublets were fitted using a Voight function with 20% Lorentzian character. Additional data for the curve fitting of the V 2p doublets include: (i) spin–orbit separation 7.2 eV, and (ii) V $2p_{1/2}$/V $2p_{3/2}$ intensity ratio 0.5.

3. Results

3.1. Catalytic behavior

Let us first explore the catalytic features of the solid studied. This will guide the characterization efforts aimed at understanding the promoting effects of cobalt for the oxidation of *n*-butane to maleic anhydride.

Fig. 1a–c shows the activity, selectivity and molar yield of the Co-impregnated catalysts. Note that those with high Co concentration are the best at low reaction temperatures while the opposite occurs at the high temperature end. This is the result of opposite trends in activity and selectivity, i.e. increasing the cobalt concentration generally increases activity while decreasing selectivity. Note that the high loading catalysts reach 80% conversion at ca. 660 K. At higher conversions the selectivity drops sharply due to increased combustion of maleic anhydride. Fig. 1d shows the selectivity dependence on conversion. Note that the low loading catalysts show near constant selectivities while the unpromoted and high loading solids exhibit the expected decrease with increasing conversion.

3.2. The structures of precursors and catalysts

Table 1 summarizes the XRD data of the VPO and Co-impregnated VPO precursors. The only phase

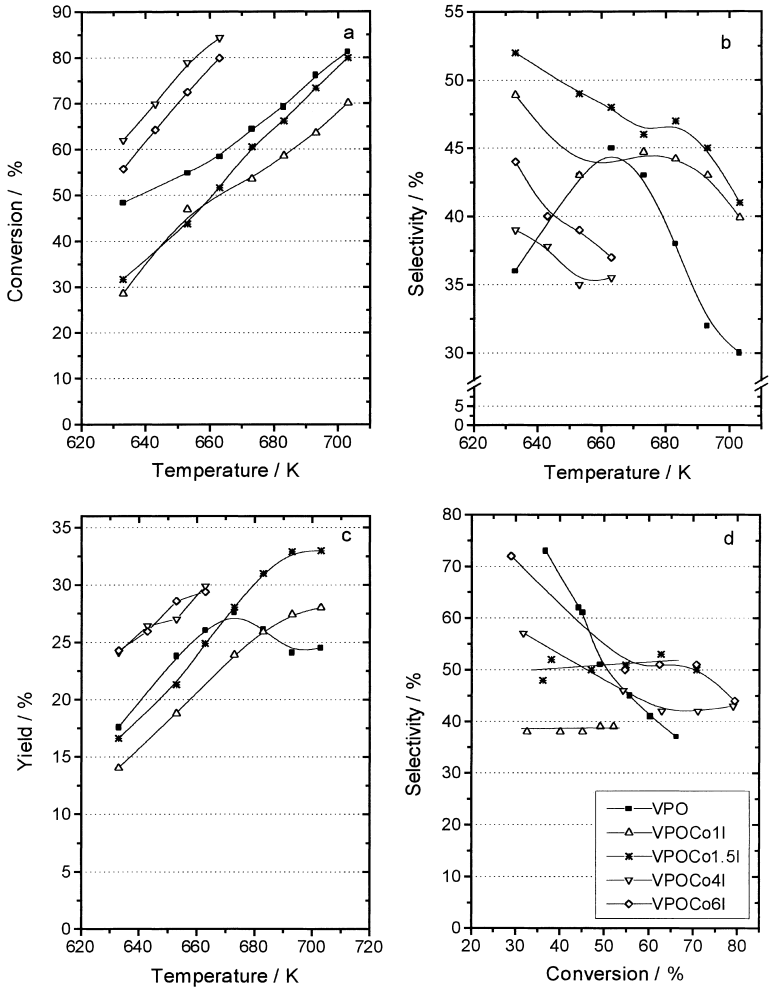

Fig. 1. Catalytic behavior of equilibrated catalysts. Reaction conditions: (a), (b), (c): 1.5% *n*-butane/air, GHSV: 900 h^{-1}; (d) 1.5% *n*-butane/air, GHSV: 2500 h^{-1}.

Table 1
XRD and XPS data of Co-impregnated and unpromoted precursors

	$(Co/V)_{bulk}$	I_{001}/I_{130}[a]	FWHM[b] (0 0 1)	FWHM[c] (1 3 0)	$(P/V)_s$[d]
VPO	–	0.41	1.0	0.31	2.15
VPOI[e]	–	0.37	0.98	0.30	2.80
VPCo1I	0.03	0.39	1.0	0.31	2.20
VPCo1.5I	0.05	0.38	1.0	0.27	2.6
VPCo2I	0.07	0.33	1.2	0.29	2.40
VPCo4I	0.13	0.37	1.14	0.28	3.70
VPCo6I	0.19	0.55	0.92	0.33	3.80

[a] Relative peak intensities (height ratios).
[b] Full widths at half maximum of (0 0 1) reflection.
[c] Full widths at half maximum of (1 3 0) reflection.
[d] Surface P/V ratios, calculated from XPS data.
[e] Unpromoted catalyst after isobutanol evaporation.

Table 2
XRD and XPS data of non-equilibrated catalysts

	I_{200}/I_{042} [a]	FWHM[b] (2 0 0)	FWHM[c] (0 4 2)	$(P/V)_s$
VPOA	0.41	1.2	0.45	2.9
VPCo1IA	0.43	2.1	0.42	3.8
VPCo2IA	0.42	1.7	0.41	2.9
VPCo4IA	0.40	2.2	0.37	3.0
VPCo6IA	0.49	1.4	0.38	3.2

[a] Relative peak intensities (height ratios).
[b] Full widths at half maximum of (2 0 0) reflection.
[c] Full widths at half maximum of (0 4 2) reflection.

detected in all cases was the vanadyl hydrogen phosphate hemihydrate. No structural modifications could be detected even in the case when 6% cobalt was impregnated on the VPO precursor.

The data obtained with non-equilibrated and equilibrated catalysts are shown in Tables 2 and 3. In all cases the only phase detected was vanadyl pyrophosphate. The main peaks correspond to the (2 0 0) and (0 4 2) reflections. The FWHMs of these peaks and their height ratios are reported. In general the (2 0 0) reflection FWHMs of the equilibrated solids are smaller than in the non-equilibrated ones while the stacking order reflected by I_{200}/I_{042} remained unchanged. Raman spectroscopy is more sensitive than XRD to detect the possible formation of minor amounts of V(V) phases. Fig. 2 shows the enlarged Raman spectra of several non-equilibrated solids. All of them exhibit the bands of $(VO)_2P_2O_7$ at 927, 1191, and 1140 cm^{-1}, in agreement with those reported by Guliants et al. [27]. Note, however, the presence of bands at 1090 and 990 cm^{-1} in VPCo1IA and at 1020 cm^{-1} in VPCo6IA. These bands indicate that the δ- and α_1-$VOPO_4$ phases are present in these non-equilibrated solids. The other non-equilibrated solids do not show any signal belonging to V(V) phases. None of the equilibrated catalysts contain $VOPO_4$ phases. A typical spectrum is shown in Fig. 2 (VPCo6IU).

3.3. Cobalt species evolution

The IR spectra of the precursors in the 1300–1900 cm^{-1} region are shown in Fig. 3. They were obtained using fluorolube as a diluting agent in order to explore the high wave number region. All of them show the characteristic vibrations of the vanadyl hydrogen phosphate hemihydrate. The band centered at 1640 cm^{-1} is characteristic of coordinated water as expected from the crystalline structure. The C=C vibrations in the plane of the aromatic ring (1450, 1492 and 1509 cm^{-1}) are also observed. The origin of these bands was investigated in a previous work [28]. They are due to benzyl alcohol and benzaldehyde retained in the solid even after drying.

In the VPCo4I spectrum (Fig. 3), a wide band at 1564 cm^{-1} and another at 1430 cm^{-1} are observed. They are coincident with the most intense ones of cobalt acetate and belong to the asymmetric and symmetric stretching vibrations of the C=O bond. This

Table 3
XRD and XPS data of equilibrated catalysts

	I_{200}/I_{042} [a]	FWHM[a] (2 0 0)	FWHM[a] (0 4 2)	$(P/V)_s$ [b]
VPOU	0.46	1.20	0.38	2.8
VPCo1IU	0.47	1.30	0.29	2.8
VPCo1.5IU	0.51	1.20	0.36	2.6
VPCo4IU	0.54	1.10	0.38	3.0
VPCo6IU	0.53	1.21	0.35	3.5

[a] See footnotes a, b, c of Table 2.
[b] Surface P/V ratios from XPS data.

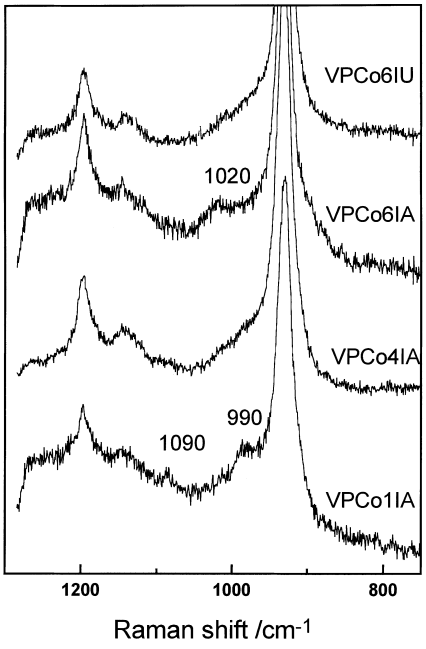

Fig. 2. Raman spectra of equilibrated (U) and non-equilibrated (A) catalysts.

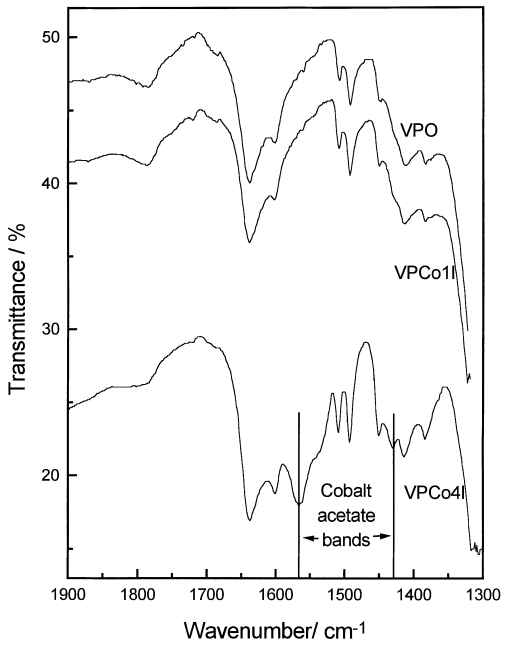

Fig. 3. FT-IR spectra of VPO, VPCo1I, VPCo4I precursors.

indicates that the solids with 4% or more, of impregnated cobalt still contain the acetate after drying. On the other hand, catalysts do not exhibit these two bands. It is a well-known fact that cobalt oxides can be detected through IR spectroscopy [29]. Experiments performed using KBr failed to show the presence of either oxides or other segregated cobalt phase.

The VPO solids were subjected to temperature-programmed reduction, in another effort to detect strong VPO–Co interactions. The TPR profiles of equilibrated and non-equilibrated solids are shown in Fig. 4. The TPR traces of non-equilibrated catalysts (Fig. 4a) show wide peaks centered at 570–600 K. This is a characteristic feature exhibited by cobalt oxides. The hydrogen consumption accounts for only 40% of the cobalt present in the samples. The TPR profiles of the equilibrated catalysts are absolutely different (Fig. 4b) showing in all cases peaks at much higher temperatures (ca. 1000 K), symptomatic of the presence of less reducible Co-containing species. Assuming a vanadium reduction stoichiometry of V(IV) to V(III),

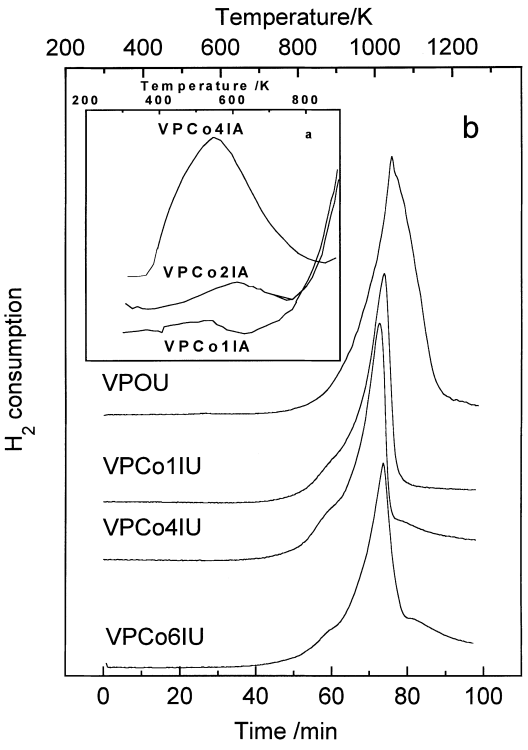

Fig. 4. Temperature-programmed reduction patterns of (a) non-equilibrated and (b) equilibrated catalysts.

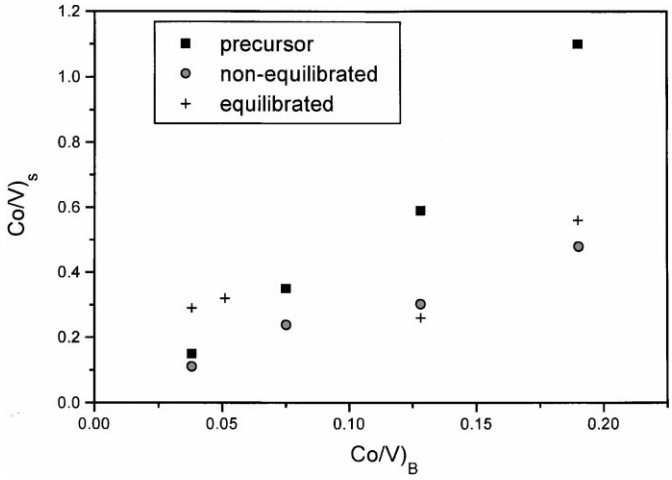

Fig. 5. Surface Co/V ratios, calculated from XPS data, as a function of the bulk Co/V ratios for impregnated catalysts.

the hydrogen consumptions for VPOU and VPCo4IU were similar. This would indicate that cobalt did not affect the reducibility of equilibrated catalysts.

3.4. The surface of Co-impregnated VPO

Fig. 5 shows the evolution of (Co/V) calculated from the XPS data when the Co bulk content increases. Both precursors and non-equilibrated catalysts show linear correlationships between $(Co/V)_s$ and the bulk concentration of Co. In the equilibrated catalysts a higher scattering is observed.

The precursor $(P/V)_s$ data shown in Table 1 indicates that the Co addition leads to phosphorus surface enrichment. This effect is, however, less significant in both non-equilibrated and equilibrated catalysts (Tables 2 and 3).

The oxidation states of vanadium on the surface of VPO catalysts has been a highly controversial matter for the last few years (vide ultra). The results obtained through curve fitting of the spectra in the V 2p–O 1s region are summarized in Table 4. In all the cases studied, the curve fitting leads to a single, well-defined binding energy for V $2p_{3/2}$ (517.7±0.1 eV) assigned to V(IV) in agreement with the values reported by López Granados et al. [17] for unpromoted catalysts.

An additional method to find out the vanadium oxidation state is based on the difference in the BEs of the O 1s and V $2p_{3/2}$ signals [Δ(O 1s–V $2p_{3/2}$)]. This method avoids the use of a reference as we concluded in a previous study [16]. Table 4 shows that all the equilibrated catalysts give Δ values of 14.3±0.1 eV. Coulston et al. [30] have reported a correlationship between the Δ value and the average vanadium oxidation state. These values are reported in the last column of Table 4 for comparison with the results obtained from curve fitting. These calculated values are all around 4. This approach also supports the overwhelming pres-

Table 4
The surface vanadium oxidation state of the equilibrated catalysts

Solids	O 1s		V $2p_{3/2}$[a]		Δ[O 1s–V $2p_{3/2}$] (eV)	V_{ox}[b]
	BE (eV)	FWHM	BE (eV)	FWHM		
VPOU	532.2	2.6	517.9	2.3	14.3	4.09
VPCo4IU	532.2	2.7	517.8	2.2	14.4	4.03
VPCo6IU	532.2	2.7	517.7	2.1	14.5	3.96

[a] Binding energies determined by curve fitting using the Googly software.
[b] Using the following correlation: $V_{ox}=13.82-0.68$ (Δ[O 1s–V $2p_{3/2}$]) from Coulston et al. [30].

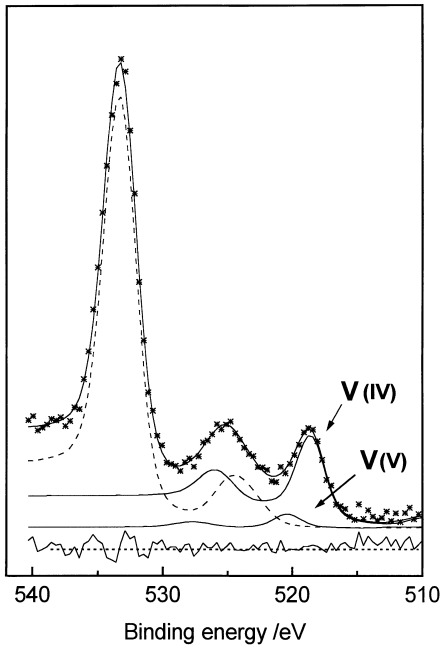

Fig. 6. XPS spectrum of equilibrated VPCo6IU catalyst in the O 1s–V 2p region and its curve-fitting results, after oxygen treatment at 623 K.

ence of V(IV) on the surface of the VPO equilibrated catalysts.

To verify our ability to detect low concentrations of surface V(V), the solids were treated with flowing oxygen at 623 K in the pretreatment chamber of the ESCA spectrometer. The VPO and VPCo6I equilibrated catalysts were used for these studies. The data pertaining to the former are shown in Fig. 6. In both cases roughly 10% V(V) was detected upon oxidation. The O/V ratios increased after oxidation from 6.9 and 9.2 to 12.6 and 14.2 for VPO and VPCo6I, respectively. However, the P/V ratio remained fixed in both cases at 2.7 and 3.4.

4. Discussion

The catalytic data (Fig. 1a–c) show that the VPO solids impregnated with 4–6 wt.% Co exhibit the best maleic anhydride yields at temperatures lower than 670 K. Note that this applies to equilibrated catalysts. The selectivity dependence upon conversion (Fig. 1d) is similar to that observed by Albonetti et al. [31] when they compared non-equilibrated and equilibrated unpromoted catalysts. Albonetti et al. assigned their fairly constant selectivity with conversion to the presence of two parallel reactions (one selective to maleic anhydride, and the other unselective). The high selectivity (extrapolated to zero conversion) suggests that at low temperature the surface sites are highly selective to maleic anhydride formation, and at high conversion, the formation of CO_x is preferred.

Let us see now how the cobalt impregnation affects the crystalline structure, the formation of other phases and the surface features of the VPO catalysts.

4.1. Structural effects

The $VOHPO_4{\cdot}0.5H_2O$ structure is highly disordered (Table 1). This may be connected to the high P/V bulk ratio as pointed out by Guliants et al. [27]. This feature is carried through to the pyrophosphate catalyst after 150 h on stream in agreement with the data shown in Table 2. Note, that despite the high P/V ratio (1.26) no $VO(H_2PO_4)_2$ was detected in any of the solids prepared.

The vanadyl pyrophosphate produced through fast, standard activation of these precursors were not contaminated by any other crystalline phase. The crystal size and the degree of stacking faults of the pyrophosphate are evaluated through the full width at half maximum of the (2 0 0) peak and the ratio of intensities of the (2 0 0) and (0 4 2) reflections [3,27,32]. The decrease in the FWHM of the (2 0 0) reflection with time on stream indicates that the thickness of the particles in the (1 0 0) direction increases (Table 3). The FWHM of the (0 4 2) peak changes slightly, reflecting a constant crystalline order of the bc plane, as well.

Ye et al. [33] studied a series of promoted VPO catalysts, prepared by the impregnation of $VOHPO_4{\cdot}0.5H_2O$ with solutions containing promoting elements. When the aqueous solutions were used, a high preferential exposure of the (2 0 0) plane was observed. They correlated the turnover frequency with the disorder along the (2 0 0) plane and they concluded that the structure of vanadyl pyrophosphate seems to depend on various factors, including the added promoter. They suggested that the promoter metal cations would be incorporated into the interlayer spacing to reduce the bonding interconnecting the layers. In our promoted catalysts no structural

changes were detected upon impregnation with cobalt acetate dissolved in isobutanol.

4.2. Formation of other phases

Several authors have reported the presence of other phases in low proportions [25,27] together with the major phase $(VO)_2P_2O_7$. Could the Raman spectroscopy reveal the presence of these minor phases that are undetectable in our catalysts by both XRD and FT-IR? The Raman spectra of certain non-equilibrated catalysts do show the presence of vanadyl orthophosphate (Fig. 2). The bands at 990 and 1090 cm^{-1} belong to the main signals of α_{II}-$VOPO_4$, while the 1020 cm^{-1} band might indicate the presence of the X1 phase reported by Koyano et al. [11]. However, the same precursors maintained on stream for more than 400 h produce solids containing vanadyl pyrophosphate only (see Fig. 2). These findings coincide with the observations made by López Granados et al. [17] with unpromoted VPO preparations. They found that the non-equilibrated catalysts contained small amounts of γ-$VOPO_4$ which disappeared after equilibration.

The presence of Co in our formulations did not induce the formation of other crystalline phases in the equilibrated catalysts. This is at variance with the results reported by Hutchings et al. [26] who reported that in one case, the proportion of V(V) phases increased with % Co addition, whereas in the other case it was just the opposite. This opposite behavior was assigned to the different preparation methods used.

No cobalt-containing phases were detected by the three techniques used: XRD, FT-IR or LRS. The cobalt acetate still present (Fig. 3) after drying the solids with cobalt loadings of 4 and 6% after drying, rapidly disappeared after a short time on stream (Fig. 3). However, TPR yielded some interesting data. The fast activated, non-equilibrated solids exhibit low temperature reduction peaks at 570–600 K (Fig. 4a). This is symptomatic of the presence of cobalt oxides easily reducible at low temperatures. These cobalt oxides disappear completely after equilibration and do form less reducible Co phases undetectable by other techniques. Hutchings [14] proposed that the promoters at high promoter/vanadium atomic ratios, act as phosphorus scavengers by either formation of metal phosphates or by formation of solid solutions. When the solid solution of the $((VO)_{1-x}M_x)_2\ P_2O_7$ type is formed, this ensures that the active catalyst compound contains the excess phosphorus required to maintain its stability in an oxidizing environment. Promoter compounds present in the solid solution could therefore play a role in maintaining the overall oxidation state of the catalyst surface. In agreement with our results, Hutchings and Higgins [25] have more recently reported that the XRD patterns do not even hint the formation of solid solutions at low promoter ratios, $M/V \leq 0.12$.

Low levels of Co, Cu, Ni were all found to give decreased maleic anhydride yields. Mc Dermott [34] also investigated the role of post deposition of promoters by impregnation on the catalyst precursor. Beneficial effects are indicated for this procedure, i.e., lower operating temperatures giving higher yields. A similar effect is observed with VPCo4I and VPCo6I (Fig. 1c). This may originate from the accumulation of the promoter on the catalyst surface, since the impregnation procedure would be expected to deposit the promoter preferentially on the surface.

4.3. Surface features of cobalt-impregnated solids

Through the use of XPS we tried to detect modifications on the catalyst surface produced by the addition of cobalt. Using both curve fitting and the correlation proposed by Coulston et al. [30], it was concluded that only V(IV) was present on the surface of the equilibrated catalysts (Table 4). The treatments at high temperatures in flowing oxygen showed that the V(IV) species are very stable under these conditions (Fig. 6). The P/V ratio of all the preparations under study was higher than the stoichiometric one and this favored the stabilization of V(IV) [9].

Our results agree with those of López Granados et al. [17] on unpromoted VPO equilibrated catalysts. Koyano et al. [11], albeit studying non-equilibrated catalysts, found by XPS only V(IV) species on the surface of those formulations made up exclusively of vanadyl pyrophosphate. On the other hand, Hutchings et al. [26] showed results at variance with our observations and those of other groups. They reported a correlation between the proportion of surface V(V), also determined by XPS, and the selectivity to maleic

anhydride in catalysts promoted with Co. Note, however, that they made these studies using promoted catalysts held on stream for 78 h, too short a period to produce an equilibrated solid.

The catalytic activity increased with the percentage of impregnated cobalt. This finding seems to indicate that the presence of high amounts of the promoter enhances the activity and somehow reduces the selectivity of the equilibrated catalysts.

5. Conclusions

No structural effects on equilibrated impregnated catalysts were detected through XRD. The non-equilibrated catalysts contain cobalt oxides which react with the VPO solids while on stream to yield a hard-to-reduce Co-containing system (Fig. 4). Whatever the Co–VPO interaction might be it is undetectable through the techniques used in this study.

The addition of Co, however, significantly increases the overall activity while slightly decreasing the maleic anhydride selectivity (Fig. 1). This seems to correlate with the increased exposure of cobalt (VPCo6I) on the catalyst surface. All this applies to equilibrated catalysts.

Non-equilibrated unpromoted VPO and those containing small percentages of Co show V(V) phases present in low proportions. Anyway, after several 100 h on stream, the only phase detected in all cases was V(IV) vanadyl pyrophosphate.

Data obtained with non-equilibrated catalysts may lead to erroneous conclusions if they are believed to be representative of what occurs during the steady state operation of industrial catalysts.

Acknowledgements

The authors wish to acknowledge the financial support received from CONICET (PIA 6313), ANPCyT (PICT No. 14-00000-00719) and UNL (CAI+D ’96 Program). They are also grateful to the Japan International Cooperation Agency (JICA) for the donation of the major instruments used in this study. Thanks are finally given to Prof. Elsa Grimaldi for the edition of the English paper.

References

[1] M. Chaar, D. Potel, M. Kung, H. Kung, J. Catal. 105 (1987) 88.
[2] K.W. Ueda, Y. Moro-oka, Appl. Catal. 70 (1991) 175.
[3] G. Centi, F. Trifirò, J. Ebner, V. Franchetti, Chem. Rev. 88 (1988) 55.
[4] B.K. Hodnet, Catal. Today 1 (1987) 527.
[5] E. Bordes, Catal. Today 1 (1987) 499.
[6] E. Bordes, Catal. Today 16 (1993) 27.
[7] F. Ben Abdelouahab, R. Olier, M. Ziyad, J.C. Volta, J. Catal. 134 (1992) 151.
[8] J. Johnson, D. Johnston, A. Jacobson, J. Brady, J. Am. Chem. Soc. 106 (1984) 8123.
[9] L. Cornaglia, C. Caspani, E. Lombardo, Appl. Catal. 74 (1991) 15.
[10] J. Ebner, M. Thompson, Catal. Today 16 (1993) 51.
[11] G. Koyano, T. Okuhara, M. Misono, J. Am. Chem. Soc. 120 (1998) 767.
[12] E. Lombardo, C. Sánchez, L. Cornaglia, Catal. Today 15 (1992) 407.
[13] B. Pierini, G. Sola, J. Petunchi, Catal. Today 15 (1992) 537.
[14] G. Hutchings, Appl. Catal. 72 (1991) 1.
[15] G. Hutchings, I. Ellison, M. Sananes, J. Volta, Catal. Lett. 38 (1996) 231.
[16] L. Cornaglia, E. Lombardo, Appl. Catal. 127 (1995) 125.
[17] M. López Granados, J.L. García Fierro, F. Cavani, A. Colombo, F. Giuntoli, F. Trifirò, Catal. Today 40 (1998) 251.
[18] S. Bej, M. Rao, Appl. Catal. 83 (1992) 149.
[19] V.A. Zazhigalov, J. Haber, J. Stoch, I. Bacherikova, G. Komashko, A. Pyatnitskaya, Appl. Catal. 134 (1996) 225.
[20] J. Haber, V. Zazhigalov, J. Stoch, L. Bogutskaya, Y. Batcherikova, Catal. Today 33 (1997) 39.
[21] W. Cheng, Appl. Catal. 147 (1996) 55.
[22] M. Sananes, J. Petunchi, E. Lombardo, Catal. Today 15 (1992) 527.
[23] N. Harrouch Batis, H. Batis, A. Ghorbel, Appl. Catal. 147 (1996) 347.
[24] R. McCormick, G. Alptekin, H. Herring, T. Ohno, S. Dec, J. Catal. 172 (1997) 160.
[25] G. Hutchings, R. Higgins, J. Catal. 162 (1996) 153.
[26] G. Hutchings, C. Kelly, M.T. Sananés-Schulz, A. Burrows, J.C. Volta, Catal. Today 40 (1998) 273.
[27] V. Guliants, J. Benziger, S. Sundaresan, Y. Wachs, J.U. Jehng, Roberts, Catal. Today 28 (1996) 275.
[28] L. Cornaglia, C. Sánchez, E. Lombardo, Appl. Catal. A 95 (1993) 117.
[29] Y. Khodakov, J. Lunch, A. Bazin, B. Rebours, N. Zanier, B. Moisson, P. Chaumette, J. Catal. 168 (1997) 16.
[30] G.W. Coulston, E.A. Thompson, N. Herron, J. Catal. 163 (1996) 122.
[31] S. Albonetti, F. Cavani, F. Trifirò, P. Venturoli, C. Calestani, M. Lopez Granados, J.L.G. Fierro, J. Catal. 160 (1996) 52.
[32] I. Hiroshi, T. Katsuyuki, O. Toshio, M. Misono, J. Phys. Chem. 97 (1993) 7065.
[33] D. Ye, A. Satsuma, T. Hattori, Y. Murakami, Catal. Today 16 (1993) 113.
[34] J. McDermott, US Patent 4 151 116 (1979).